ELEVATED MODERN SEDIMENTATION RATES OVER THE BURIED TRINITY RIVER INCISED VALLEY SUGGEST ELEVATED, LOCALIZED SUBSIDENCE RATES, GALVESTON BAY, TX, USA,

A Thesis

by

ANDREW DAVID PEKOWSKI

Submitted to the Office of Graduate and Professional Studies of
Texas A&M University
in partial fulfillment of the requirements for the degree of

MASTER OF SCIENCE

Chair of Committee,	Timothy Dellapenna
Committee Members,	Peter Santschi
	Peter van Hengstum
Head of Department,	Shari Yvon-Lewis

August 2017

Major Subject: Oceanography

ABSTRACT

This study investigates sedimentation rates within Galveston bay, TX, and their utility in estimating differential compaction in Texas coastal plain estuaries. Most modern Texas estuaries are situated over incised Pleistocene paleo-channels up to 30 m deep, filled primarily with unconsolidated mud-dominated Holocene fluvial and estuarine deposits. The Galveston Pier 21 tidal gauge has a 100-year record which has recorded a relative sea-level rise rate 3 times the global average, and this rate is considered a regional rate. However, Pier 21 is situated over the Trinity River incised paleo-valley (TRIV). A CHIRP sub-bottom profile and multiple transects of vibra-cores were collected across the TRIV to investigate if sedimentation resulting from enhanced subsidence has increased over the TRIV compared to the TRIV flanks. Profiles of Hg and textural changes were used alongside sedimentation rates derived from excess ^{210}Pb activity to determine the recent sedimentary history of the bay. Sedimentation rates ranged from 0.34 – 1.48 cm yr^{-1}, with the highest rate being found directly over the TRIV. Correlations in Hg and textural data reveal a general deepening and extension of strata within cores collected directly over the TRIV. Analyses of the CHIRP line also reveals a localized thickening of individual stratigraphic layers within Holocene estuarine fill across the TRIV, with a thinning on the flanks. Taken together, the evidence suggests that differential compaction of the unconsolidated Holocene estuarine fill within the TRIV has produced localized, elevated sedimentation rates, suggesting

enhanced localized subsidence up to four times as great within Trinity Bay over the TRIV, than in areas adjacent to it.

ACKNOWLEDGEMENTS

I would like to thank my committee chair, Dr. Timothy Dellapenna as well as my committee members, Dr. Peter Santschi, and Dr. Pete van Hengstum for their guidance and support throughout the course of this research, and Dr. Debbie Thomas for encouraging me as an undergraduate to pursue a higher degree. I am also grateful to the Texas Sea Grant program for providing the funding for much of this project.

Thanks also go to my colleagues at Texas A&M University for making this such a great experience. Many of my trials and triumphs were shared with fellow students who I can now call lifelong friends. Their help, both mentally and physically, was vital to my success and I wish them all the best in their own accomplishments.

Thanks should also be given to the many graduate and undergraduate researchers at Texas A&M University at Galveston who contributed in some way to the project. Whether through lab processing or field work, this research required many hands to complete. I thank everyone for their eagerness and willingness to help.

Finally, thanks to my fiancée, and soon to be wife, Caitlin. Thank you for the constant comfort and reassurance on both the good days and the bad. Your continued support of this endeavor was invaluable to my success.

CONTRIBUTORS AND FUNDING SOURCES

Contributors

This work was supervised by a thesis committee consisting of Drs. Timothy Dellapenna and Peter van Hengstum of the Departments of Oceanography and Marine Sciences and Dr. Peter Santschi of the Department of Marine Sciences.

All work for the thesis was completed independently by the student**.**

Funding Sources

This work was made possible in part by an Institutional Grant (NA14OAR4170102) to the Texas Sea Grant College Program from the National Sea Grant Office, National Oceanic and Atmospheric Administration, U.S. Department of Commerce. Its contents are solely the responsibility of the authors and do not necessarily represent the official views of the Texas Sea Grant College Program.

NOMENCLATURE

^{210}Pb	Lead-210	
^{210}Pb	Radioactive Lead Isotope	
^{209}Po	Radioactive Polonium Isotope	
A_0	Initial Activity	dpm g^{-1}
A_z	Activity at Depth	dpm g^{-1}
BHD	Bay Head Delta	
Bkg-Hg	Background Mercury Concentration	ng g^{-1}
CBE	Central Basin Estuarine	
CRM	Certified Reference Material	
Hg	Mercury	
HCl	Hydrochloric Acid	
HNO_3	Nitric Acid	
HSC	Houston Ship Channel	
IPCC	Intergovernmental Panel on Climate Change	
Max-Hg	Depth of Maximum Mercury Concentration	ng g^{-1}
NOAA	National Oceanic and Atmospheric Association	
Pb	Lead	
R^2	Coefficient of Determination	
RSLR	Relative Sea-Level Rise	
SJR	San Jacinto River	

T-Hg	Total Mercury Concentration	
TRIV	Trinity River Incised Valley	
USGS	United States Geological Survey	
z	Sediment Depth	
α	Alpha Radiation	
Δ	Relative Change in Variable	
λ	Decay constant of ^{210}Pb (0.031)	$year^{-1}$

TABLE OF CONTENTS

Page

LIST OF FIGURES

Page

LIST OF TABLES

Page

1. INTRODUCTION

Modern rates of relative sea-level rise (RSLR) along the Texas coast are a product of an increasing average eustatic (global average) sea-level, regional hydro-isostatic rebound, and local rates of subsidence. It is well documented that there has been in excess of 3 m of land subsidence in the San Jacinto River/Houston Ship Channel (SJR/HSC) portion of Galveston Bay (Coplin and Galloway, 1999; Kolker et al., 2011; Lester and Gonzalez, 2002). Analyses reveals that within the SJR/HSC, sedimentation rates were as high as 1.9 cm yr^{-1} and local subsidence rates were around 2.6 cm yr^{-1}, demonstrating that although these two rates are of the same order of magnitude, that sedimentation lags behind subsidence (Al Mukiami et al., in review and Al Mukiami, 2016). These rates are in stark contrast to the eustatic sea-level rise rate of ~0.2 cm yr^{-1} (IPCC, 2013). The elevated subsidence in the SJR/HSC area is primarily a result of excessive groundwater removal (Coplin and Galloway, 1999; Kolker et al., 2011). Al Mukiami (2016) revealed that elevated subsidence can be a localized phenomenon and he proposed that within the portions of the bay overlying the paleo-Trinity River Incised valley (TRIV), subsidence may be triple that of adjacent areas. The Galveston Pier 21 tidal gauge is used as a basis for his hypothesis. This station has collected a continuous hourly water level record since 1904 CE and has recorded an average RSLR rate of 0.65 cm yr^{-1}, more than 3 times the global rate and also, one of the highest RSLR recorded for any tidal gauge in the US (NOAA, 2013). The Pier 21 RSLR has been used widely as the regional rate for the upper Texas coast (e.g. Tebaldi et al., 2012; Cox, 2002; Turner,

1991). However, the Pier 21 station sits atop the flanks of the TRIV and has experienced differential compaction of the underlying sediment (Anderson, 2007). Al Mukiami et al. (in review) and Al Mukiami (2016) estimated, based on sedimentation rates, that subsidence rates in both East and West Galveston Bay approximate the regional rate, which is one-third of the Pier 21 rate and further speculates that the remaining 0.45 cm yr^{-1} results from differential compaction of the Holocene incised valley fill. If this is correct, the elevated rate of subsidence is only very localized rather than representative of the regional rate.

Currently, Trinity Bay is a broad flat bay that contains the same depositional estuarine environment and sediment texture across most of its surface. Stratigraphically, the bay is underlain by the TRIV (Fig. 1), which formed during the last low stand in sea level through the incision of underlying indurated Pleistocene clay (Rodriguez et al., 2005). During the Holocene transgression, the valley was filled with unconsolidated sand from bay head deltas and estuarine mud (Thomas and Anderson, 1994). This provided an ideal site to test the following hypothesis: *Sedimentation rates over the TRIV are three times higher than those located in adjacent locations within the same bay environment, but not located over the TRIV, and that this will be manifested as a thickening of strata over the incised valley.*

This project focuses on quantifying subsidence due to shallow Holocene sediment compaction over the TRIV using sedimentation as a proxy for subsidence rate. Al Mukiami et al. (in review) documented that the highest rates of sedimentation and subsidence are positioned in the same areas in Galveston Bay. This is expected because

additional accommodation space is created after compaction of underlying strata. If sedimentation rates over the TRIV are higher than in areas adjacent to it, and the bay bottom has the same bathymetry, then this indicates that the TRIV is experiencing a greater rate of subsidence relative to elsewhere in the bay. If this enhanced subsidence is localized over the Trinity Incised valley, then it would strongly suggest that the enhanced subsidence is due to differential compaction of the sediment within the valley.

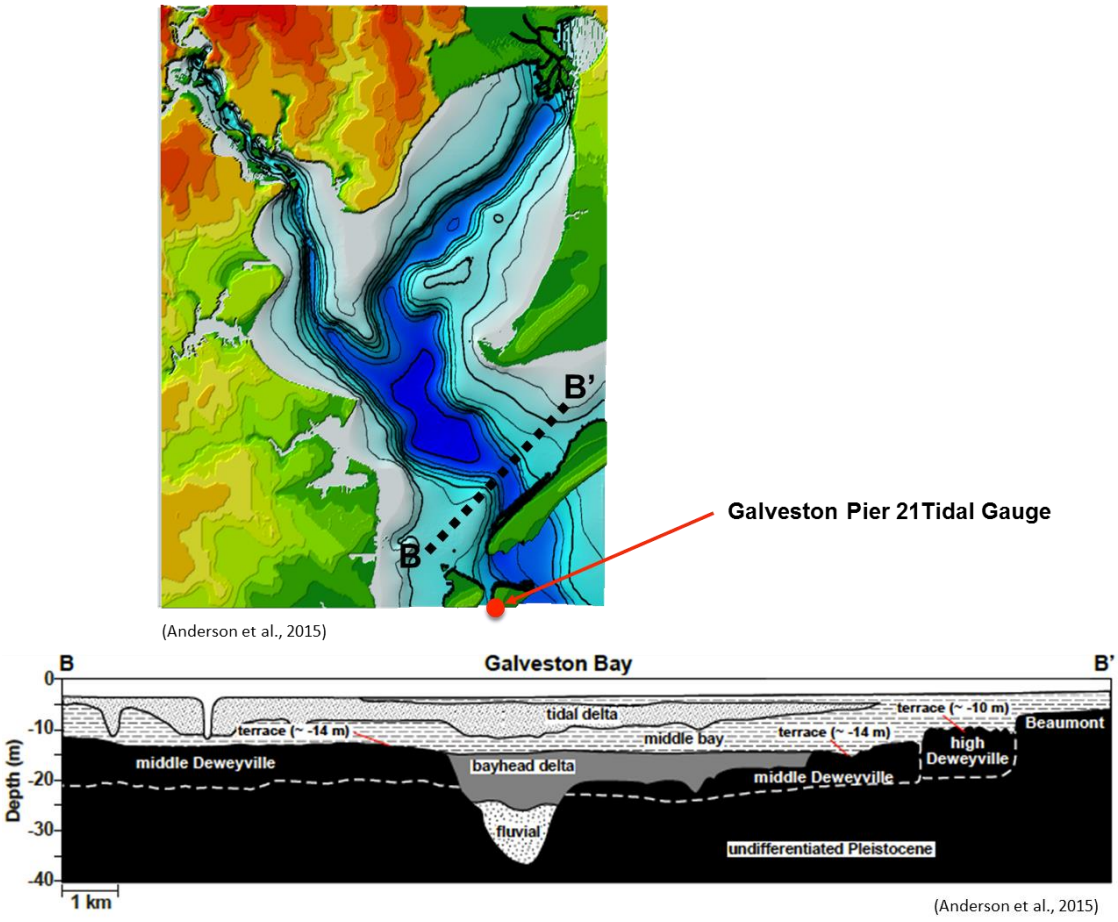

Figure 1. Structure map of the paleo-Trinity River incised valley. Cross section across valley indicates different sedimentary facies observed within Galveston Bay atop paleo terraces. Terraces increase with age away from the valley axis. Reprinted from Anderson et al., 2015.

2. BACKGROUND

2.1 Study Site and Valley Formation

All data and samples were collected within the Trinity Bay portion of Galveston Bay, Texas, USA, along the northern Gulf of Mexico. The TRIV extends directly through the center of Trinity Bay, trending approximately northeast to southwest. Trinity Bay provided the best location to measure undisturbed sedimentation due to its relatively remote location, lack of dredged navigation channels, and distance from Galveston Bay's tidal delta.

Trinity Bay is approximately 24 km long and 16 km wide containing shallow turbid waters of a mean depth of 2.5 m (Langford et al., 1969), with wave conditions depending on the strength and direction of wind. The Trinity River provides the main freshwater input in the northeastern portion of Trinity Bay. Trinity Bay is crisscrossed by multiple historical oil pipelines and submerged or protruding hazards are abundant.

The Trinity River bayhead delta is found at the northeastern end of Trinity Bay, where the Trinity River empties into the bay and sandy shorelines rim both the northwestern and southeastern bay margins. Within its central basin, Trinity Bay consists of uniformly flat, muddy central estuarine facies, with extensive (1.5 – 3 km wide) bay-margin flank shoals, consisting of muddy sand. The muddy central estuarine facies stratigraphically sits atop unconsolidated bay head and floodplain deposits, which sit atop the Pleistocene unconformity. Below this unconformity resides the hard indurated

Pleistocene-aged Beaumont Clay and fluvial Deweyville Terraces, which form the flanks of the TRIV. These terraces are a result of downcutting during the last fall in sea level, resulting in cross-sectional profiles that vary across the incised valley (Blum et al., 1995; Morton et al. 1996; Blum and Price 1998). In Previous studies, terraces within Trinity Bay have been extensively mapped (Blum et al. 1995; Morton et al. 1996). The variable depths at which the terraces now reside have permitted sediment accumulation of varying thicknesses across the valley, providing evidence for the possibility of localized differential compaction.

Sediment supply to Trinity Bay is predominately from the Trinity River. Damming of the Trinity River began in 1911 and now includes 31 major dammed reservoirs, each acting as a sediment trap. It is expected that over time sediment supply, and therefore sedimentation, would be reduced both downriver and in the bay. While the bay itself has been buffered from some of this sediment reduction due to significant alluvial storage of sediment in the lower Trinity River, a reduction in suspended sediment load has been recorded, particularly after the 1968 construction of the Lake Livingston Dam (Ravens et al., 2009).

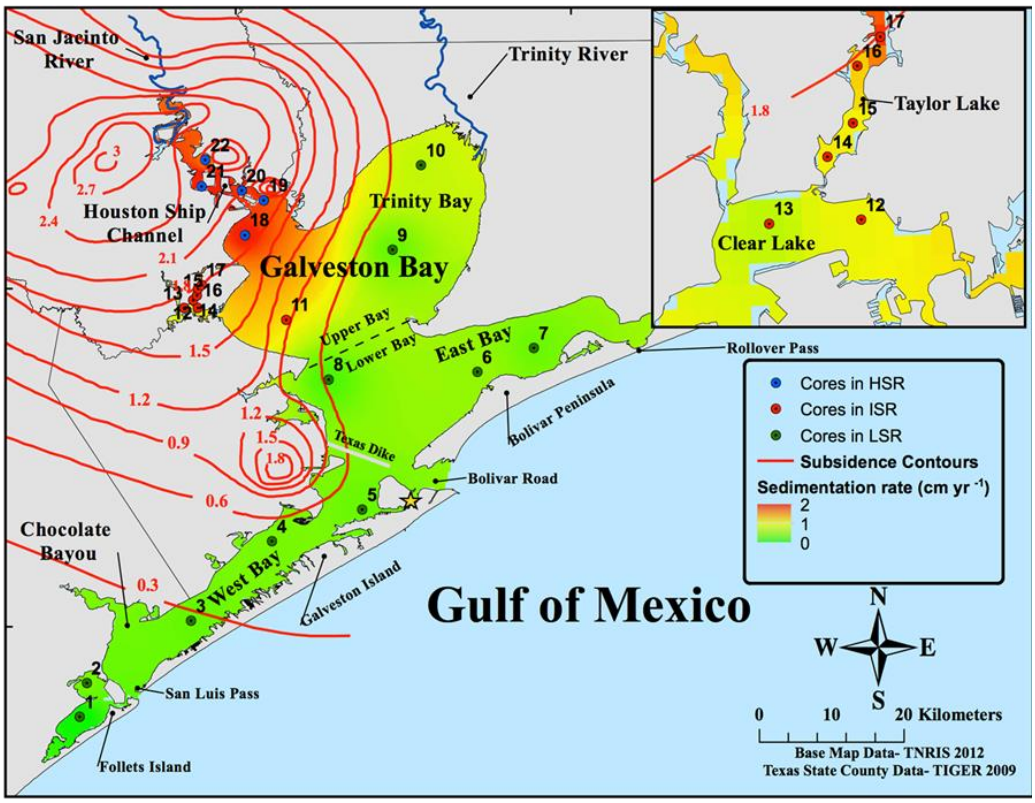

Figure 2. Detailed map of study area in Al Mukaimi (2016). Coring locations marked and categorized as being in either a Low Subsidence Region (LSR), Intermediate Subsidence Region (ISR), or a High Subsidence Region (HSR). Contour plot represents subsidence from 1906 to 2000 (HGD, 2008). Interpolated average sedimentation rates determined through ^{210}Pb and ^{137}Cs geochronology. Yellow star indicates location of the Pier 21 tidal gauge.

2.2 Previous Work

Findings presented in Al Mukiami et al. (in review) and Al Mukiami (2016) motivated much of this project. Using ^{210}Pb and ^{137}Cs geochronology, Al Mukiami measured a drastic variation in sedimentation rates within Galveston Bay that ranged

from 0.05 – 1.90 cm yr^{-1} (Fig. 2). High rates of sedimentation were found in areas that were experiencing a similarly high rate of subsidence, which was concentrated in the SJR/HSC portion of the bay. While the two rates were found to be of a similar order of magnitude, sedimentation rate lagged behind subsidence, creating an accretionary deficit in areas where subsidence was highest. Larger deficits would lead to bay deepening and a higher rate of RSLR.

Other studies have reported a wide range of sedimentation rates within Galveston Bay including early measurements by Rehkemeber (1969) who reported a sedimentation rate for the entire Galveston Bay of 0.35 cm yr^{-1} from 30 borings collected throughout the bay and radiocarbon dating. Santschi et al. (2001) reported a sedimentation rate of 0.38 cm yr^{-1} within Trinity Bay through the use of $^{239,240}Pu$ activity. Later, White et al. (2002) reported a sedimentation rate of 0.50 cm yr^{-1} occurring in the Trinity River bayhead delta, near the site of this study and an area with a rate of measured subsidence (1.10 cm yr^{-1}). In portions of West Galveston Bay where subsidence is also elevated, sedimentation rates were reported as approximately 0.2 cm yr^{-1} from radionuclide analysis (Ravens et al., 2009), showing that an increased rate of sedimentation due to subsidence is dependent on an ample supply of sediment to fill accommodation space.

Seismic mapping of the TRIV has previously been completed with great detail through multiple studies and compiled by Rodriguez et al. (2005). The valley architecture is generally well documented, however these studies focused on larger scale regional stratigraphic questions and did not address causes of subsidence or other localized issues. In addition, considerable effort has gone into addressing

anthropogenically induced subsidence surrounding the Houston metropolitan area (Coplin and Galloway, 1999; Michel, 2006; Yu et al., 2014), but so far, no studies have addressed subsidence driven by differential compaction within the bay.

2.3 Subsidence

Subsidence, which is most easily defined as a sinking of the ground relative to sea level, can occur when unconsolidated sediment is compressed by the overburden placed upon it by overlying sediment. Historically, subsidence in the Houston-Galveston area is the result of fluid removal triggering both the compression of deep aquifers and movement along shallow sub-surface faults (Yu et al., 2014; White and Morton, 1997). The increased withdrawal of water, oil and gas throughout the region over the last several decades has caused a drastic increase in the rate of subsidence (Michel, 2006; Ewing 1985; Yu et al., 2014), leading to an increased frequency of flooding and extensive wetland loss, as well as widespread damage to local infrastructure. The creation of entities such as the Fort Bend, Harris and Galveston County Subsidence districts has reduced the rate of subsidence along Houston's east coastal plain through strict water management policies, yet subsidence has accelerated in areas of rapid growth in northwest portions of Houston (USGS, 2002).

It is hypothesized in this study that subsidence in Trinity Bay is primarily a result of the consolidation of shallow marine sediment. We base this speculation on the observation that Trinity Bay is distal from the main epicenters of fluid withdrawal

induced subsidence that has so far been observed and documented. A large volume of sediment has accumulated in the central portions of Trinity Bay because of the TRIV's deep thalweg (Rodriguez et al,. 2005). It is expected that the greater weight of sediment will cause a collapse of pore space in the deposited sediment particles, removing fluid and compacting the unconsolidated sediment. This would create a greater rate of subsidence in the central portions of the bay, directly over the valley, than in shallower areas of the valley where less sediment has accumulated and the Holocene strata is thinner.

Much of the land surrounding Galveston Bay sits at or near sea level, with coastal plains sloping only gently away from the coast making the region particularly prone to flooding events that occur as the result of unseasonably high rains or hurricanes. Actively monitoring subsidence, which is historically performed using borehole extensometers and GPS benchmark stations, is becoming increasingly important as Houston continues to grow. No monitoring of subsidence within the open bay is currently being performed.

2.4 Hg Analysis

Industrialization surrounding the Galveston Bay area throughout the last century has caused an increase in the release of trace metals (e.g. Hg) into the environment and their input has been recorded in the sediment record. Significant shifts in concentration

at depth can be correlated to the known historical input of contaminants into the bay. Input of Hg into Galveston Bay has been well documented by Al Mukaimi (2016) and has been proven to be a valuable geochronology tool for estimating sedimentation rates within the bay through the use of known chronohorizons. The input history of Hg is well established (Al Mukaimi, 2016) and measurement of Hg within sediments is easy and can be performed quickly. Hg profiling of sediment cores is used in this study to better constrain sedimentation rates and to add redundancy in our other geochronology measurements.

Hg occurs naturally in the environment from the weathering of Hg bearing rocks and volcanic emissions (Bank, 2012), but is also introduced anthropogenically into Galveston Bay from both atmospheric fallout stemming from the burning of fossil fuels and through direct release of contaminants into the bay (Bank, 2012; Liu et al., 2012). Input of Hg above background levels began in the early 1900's, became dramatically elevated around 1940 due to increased petroleum refining and peaked in the 1960's. Given this information, along with Hg's affinity for accumulating in sediment, the downcore peak in Hg concentration can be used to identify the two separate chrono-horizons, onset of industrial use in 1900, where its concentration rises above a background level of 20 ng/g and elevated input in 1940.

3. METHODS

3.1 Data Collection

Field data and samples were collected through a series of research cruises during the summer of 2016 and winter of 2017, aboard the R/V *Big Daddy*, a 7.9 m long aluminum motorized coring barge, rigged with a bow mounted A-frame. Field work depended on calm bay conditions for proper data acquisition aboard the small vessel.

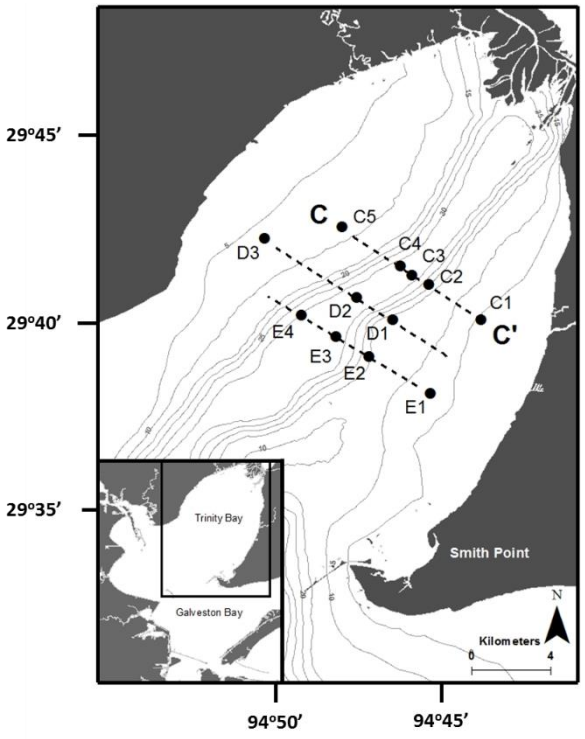

Figure 3. Field map of Trinity Bay showing coring locations (black dots) and seismic transects (dotted lines). Line C to C' was the only usable seismic transect. Contour map of Pleistocene surface of TRIV shown under coring locations.

Using *Rodriguez (2005)* as a starting point, a seismic profile (designated Line C) was collected across the TRIV using an Edgetech® 216 Full Spectrum Sub-bottom CHIRP seismic system (Figure 3). The CHIRP system was towed alongside the R/V Big Daddy while travelling at approximately 3 – 4 knots (5.6 – 7.4 kph) and operating at a frequency of 10 kHz, resulting in a penetration of up to 20 m into the seabed. This seismic profile provided a northwest to southeast trending (along strike) cross sectional image of the bay deposits, allowing for the visualization of the TRIV within the bay. Two additional seismic lines were collected, but acquisition was marred by worsening weather conditions, resulting in very low resolution profiles unusable for the study. Limited access to working equipment and certified vessel operators precluded additional data acquisition. CHIRP data acquisition and processing was accomplished using Chesapeake SonarWIZ.Map® software.

Locations for vibra-cores were chosen based off visual inspection of the seismic profiles (Fig. 3). Upon delineation of the incised paleo-valley, cores were collected along the seismic transects. This permitted comparison of rates of sedimentation from locations of varying unconsolidated sediment thicknesses across the TRIV. In total, 12 vibra-cores were collected in Trinity Bay using 2 m-long core barrels with a diameter of 7.62 cm (3 inches), with the goal of sampling approximately the last 100 years of sedimentation. Cores were collected using a PVL-Technologies® submersible vibrating coring head deployed from the bow mounted A-frame on the R/V *Big Daddy*. These cores ranged from 0.9 – 1.5 m length of actual core retrieval. Only 5 of the 12 cores were collected along the pre-collected seismic profile, the rest were collected on two separate

transects of the TRIV to the southwest of our single seismic profile, along the two profiles with diminished quality of seismic reflection data.

3.2 Data Processing

Processing of the sub-bottom profile consisted of applying various gain settings offered through the SonarWiz program to optimize image clarity. The sediment-water interface (mudline) was identified and a single underlying continuous horizon was traced and identified. Only one other feature was partially visible below this mapped horizon.

Core locations were chosen over areas where the single mapped horizon had both thicker and thinner overburden to compare areas of differing potential shallow compaction. Upon collection, cores were split length-wise and immediately digitally photographed, described, and x-radiographed. Subsampling at predetermined 1-cm intervals occurred immediately after to insure minimal evaporative loss of water content. Samples were placed into small pre-weighed tins and then placed directly into an oven set to 70^{o} C for 24 hours to dry. Samples were weighed before and after drying to determine water content. The mud fraction of these samples were then obtained through wet sieving using a 63 μm sieve for use in short-lived radioisotope geochronology. Downcore grain size analyses were conducted on a separate sub-sample from the core using a Malvern Masterizer 2000 laser diffraction particle size analyzer. An archived half of each core was carefully stored in a large core repository refrigerator for future examination.

Core	Date Collected	Coordinates		Core Length (cm)
C1	June 20th, 2016	29 39.492 N	094 43.792 W	123
C2	June 20th, 2016	29 40.450 N	094 45.217 W	131
C3	July 20th, 2016	29 40.715 N	094 45.620 W	149.5
C4	July 20th, 2016	29 40.958 N	094 45.997 W	136
C5	July 20th, 2016	29 42.015 N	094 47.584 W	107.5
D1	July 20th, 2016	29 37.489 N	094 45.175 W	89
D2	July 20th, 2016	29 38.486 N	094 46.840 W	87
D3	July 20th, 2016	29 39.034 N	094 47.744 W	111
E1	July 20th, 2016	29 39.611 N	094 48.685 W	125
E2	July 20th, 2016	29 39.491 N	094 46.205 W	133
E3	July 20th, 2016	29 40.088 N	094 47.183 W	73
E4	July 20th, 2016	29. 41.714 N	094 49.687 W	143.5

Table 1. Information about collected cores.

3.3 Hg Analysis

The analysis of total mercury concentration (T-Hg) was completed using a Direct Mercury Analyzer (Milestone DMA-80) to maintain compliance with U.S EPA Method 7473 (*EPA, 1998*). Calibration of the DMA-80 was rigorously completed using prepared standard solutions of known Hg concentration. All calibrations were verified with certified reference material MESS-3 Marine sediment (0.091 ± 0.009 ppm, National Research Council of Canada). Approximately 150 mg of dry powdered sediment was used from pre-determined intervals throughout the core to accurately measure Hg concentration at depth. To preserve the reliability and accuracy of measurements, a

series of blanks, standards, and duplicate samples were analyzed in between study samples. Samples containing only the <63 μm (silt and clay) of sediment were used for analysis.

3.4 ^{210}Pb Geochronology

Rates of sedimentation were determined using the ^{210}Pb geochronological method (Robbins, 1978; Appleby and Oldfield, 1978; Krishnaswamy et al., 1971; Koide et al., 1972) which has been used extensively to investigate accumulation rates of marine sediments (Al Mukiami, 2016; Dellapenna et al., 1998). Activity of ^{210}Pb, a short-lived radioisotope, was measured indirectly by measuring the activity of its isotopic granddaughter, ^{210}Po, as they are assumed to be in secular equilibrium (Nittrouer et al., 1979). 1 – 2 g of the pre-obtained mud fraction from sediment samples was placed in a Teflon digestion beaker and spiked with 0.25 μl of ^{209}Po with known activity. Samples were then digested using 15 ml of concentrated HCl and HNO_3. Teflon beakers were placed into a HotBlock until samples were near dry. After near dryness, 15 ml of HCl and HNO_3 was added again to the beakers and the procedure repeated. Once the samples were near dry, 15 ml of HCl alone was added to the beakers and the drying procedure repeated. Once near dryness was reached for a third time, 50 ml of 1.5 N HCl was added to the beakers and ascorbic acid stirred in to the leachate to complex the free Fe (III). A single silver planchet, measuring 1 cm^2 with tape covering one side, was then placed in

the leachate along with a magnetic stir bar. The leachate solution was then stirred for about 24 hours, allowing both the ^{209}Po and ^{210}Po to be electroplated onto the silver planchet. After drying, planchets were counted for 24 – 48 hours using an α spectroscopy surface barrier detector. Counts of ^{209}Po and ^{210}Po were obtained and their ratio used to determine the activity of ^{210}Pb in each sample using a constant initial concentration, constant rate of supply model (CIC-CRS). A supported activity of 0.7 dpm g^{-1} was determined from constant ^{210}Pb activities at depth and applied to all cores. Anything in excess of this base line was considered unsupported activity and used in calculating a logarithmic regression line to determine sediment accumulation rates using the following equation:

$$S_{avg} = \frac{\lambda \Delta z}{\ln(\frac{A_o}{A_z})}$$

Where S_{avg} is the sedimentation rate (cm yr^{-1}), λ is the decay constant of ^{210}Pb (0.0312 yr^{-1}), Δz is the change in depth of the regression line (cm) A_o is the excess ^{210}Pb activity at the start of the regression (dpm g^{-1}), and A_z is the excess ^{210}Pb activity at the end of the regression (dpm g^{-1}). A corrected depth was used for samples along the regression line based off a calculated porosity determined from the water content measured throughout the core and an average sediment density of 2.65 g cm^{-3}. Regressions were drawn at the base of any observed surface mixed layers, indicated by an interval of constant ^{210}Pb activity at the surface of the sediment core.

4. RESULTS

4.1 Analysis of Sub-bottom Profile

The shallow penetration of the CHIRP (approx. 20 m at its deepest) did not allow for complete delineation of the TRIV. However, an acoustic reflector below the sediment surface was clearly observed and is interpreted as the top of the bay-head delta (BHD) (Rodriquez et al., 2005), which is seen here as the surface expression of the underlying valley (Fig. 4). Little can be inferred under the BHD other than in a single area where CHIRP penetration accurately captured what appears to be an underlying channel. Everything above the BHD is interpreted as the central basin estuarine facies (CBE), continuing with the nomenclature established by Rodriguez et al. (2005). Multiple pipelines were detected, appearing as strong, repeating, parabolic reflectors at depth, which caused a small loss in data acquisition below their locations.

CBE sediment is approximately 2 m thick at its thinnest point towards the edges of the bay and is composed of mostly parallel reflectors. In the central portion of the bay, directly overlying the TRIV, the CBE sediment thickens to approximately 4 m, even extending upwards of 8 m in submerged channels cut through the BHD. This change in thickness occurs sharply and the location of the change is interpreted as the flanks of an inundated terrace. The top of the central basin sediment, also interpreted as the sediment-water interface, has the strongest acoustic impedance where the sediment is thinnest.

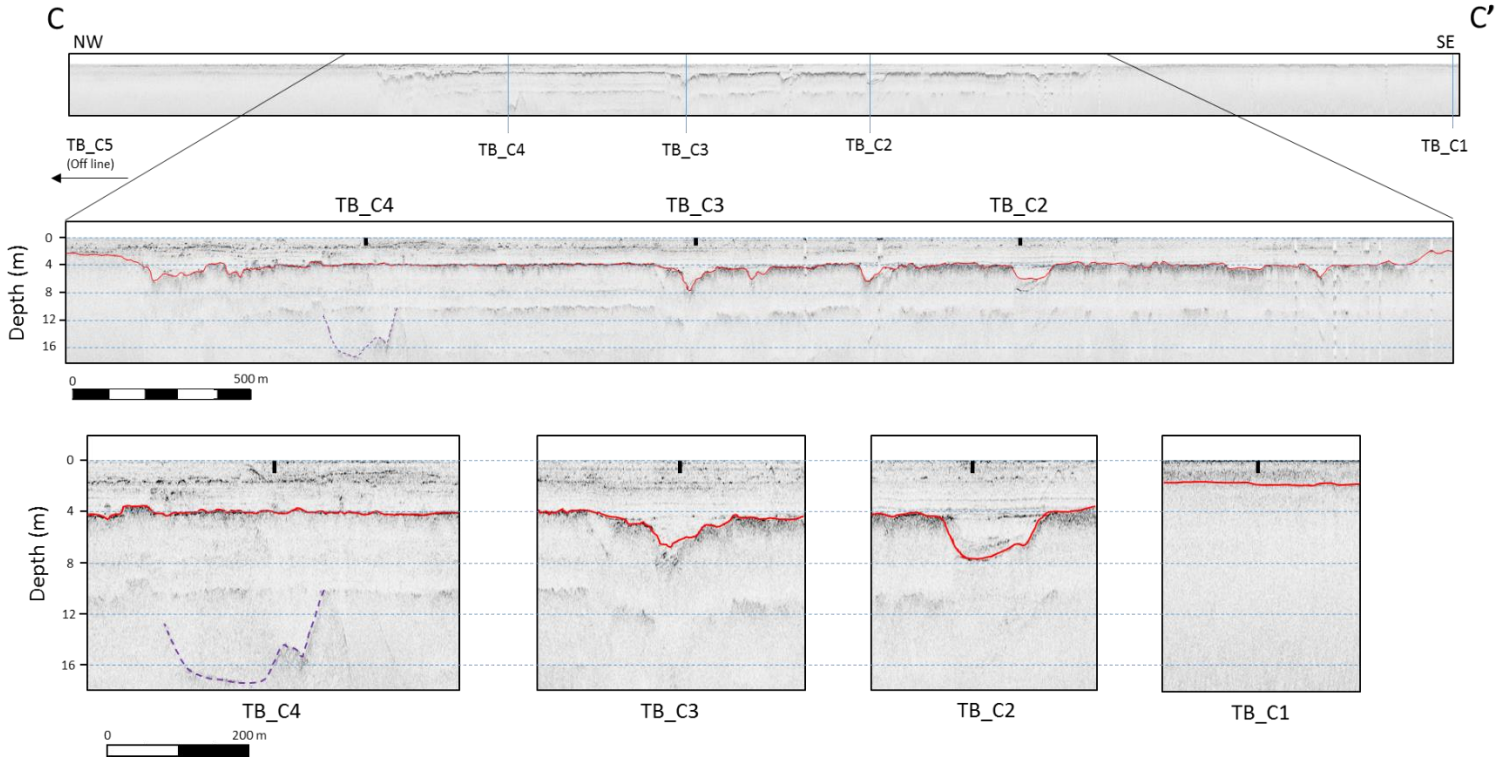

Figure 4. Sub-bottom profile of transect C of Trinity bay, collected using a CHIRP seismic system. The red line indicates a strong reflector that is determined to be the surface of the Bay Head acoustic blanket, which limited the penetration of the CHIRP. The reflector is also inferred as the surface expression of the underlying TRIV. Coring locations are displayed on profile with the exception of C5 which was take just beyond the profile and were chosen to capture sediment over areas of differing sediment thickness above the aforementioned acoustic reflector. The only future observed below this surface was directly below core C4 and is interpreted as the surface of the Pleistocene clay.

The surface of the BHD is quite variable along the transect length and is most apparent in the central portion of the bay and is almost entirely indistinguishable along the bay-margin flanks. The bay-margin flank shoals are composed of muddy sand, creating a much harder bottom, consequently, the bay-margin flank area has an enhanced acoustic impedance of the sediment-water interface reflector. Where visible, the surface of the BHD is uneven and rutted with several channels filled with central basin sediment.

Below the BHD, little can be clearly interpreted, other than a single channel approximately 12 – 16 m below the sediment-water interface. This channel is likely a portion of the TRIV surface, however, due to its poor resolution it cannot be traced further across the seismic line.

4.2 Sediment Cores

Five of the twelve cores were collected along seismic transect "C" (C1, C2, C3, C4, and C5). Cores C2, C3, and C4 were collected from locations where the central basin strata are thickest, as determined by the CHIRP data. The remaining two cores, C1 and C5, were collected on both extreme ends of the seismic line where the CBE strata is thinnest, distal from the central portions of the TRIV. Core C2 and C3 were collected directly over areas where a paleo-channel in the BHD allowed for CBE sediment to thicken while core C4 was aimed to collect sediment over the single area where the BHD was penetrated by the CHIRP and an underlying channel was exposed. Core C5 was collected just beyond seismic transect C, so no seismic data is available for this core,

though it is assumed to be very similar in characteristic to core C1 due to their distance from the TRIV.

Without proper seismic acquisition along the other two transects of the TRIV, the locations for the remaining cores were based off what little interpretations could be made from the poor-quality CHIRP data. Three cores, D1, D2, and D3, were collected across transect “D”. Cores D1 and D2 were collected just outside the TRIV and directly over the TRIV respectively, while core D5 was collected far from the TRIV near the northwest shore of Trinity Bay. Lastly, 4 cores were collected along transect E, which was located furthest from the mouth of the Trinity River. Core E1 was collected outside the TRIV, core E2 was collected just outside the TRIV, and cores E3, and E4 were collected directly over the TRIV. A comparison of coring locations to a map of the TRIV from Rodriquez et al., (2005) confirmed the cores estimated relative positions to the TRIV.

Upon splitting, a qualitative analysis of all twelve cores revealed similar grey mud with abundant shell beds. Visual core logs exposed little about the characteristics of the sediment. X-radiographs allowed for more detailed facies descriptions and revealed mostly large structureless shell beds with few planar laminae and bioturbation. Laminae were only distinguishable via x-radiographs except in core D2 where distinct black laminations were visible throughout the core and are interpreted as being organic in origin.

4.3 Sedimentology

Downcore textural variability documents a relatively consistent pattern of sedimentation throughout the study area (Fig. 5). Cores closest to the shoreline of Trinity Bay, cores C1, D3, and E1, consist of a greater proportion of coarser grains with an average d50 grain size of 76.1 μm, 38.4 μm, and 44.1 μm respectively. While at first interesting, this variation is to be expected given the proximity to the higher energy shore environment, and therefore, increased proportion of coarser particles. The remaining cores located away from the shoreline were finer grained with an average d50 grain size ranging from 5.4 μm – 20.7 μm (fine to medium silt). All cores are characterized by finer particles near the sediment water interface before coarsening with depth. Core D2 presents the largest deviation away from this pattern, consisting of fine grains with the lowest average standard deviation, which is thought to be due to its distal location from the shoreline. Generally, sedimentary structures cannot be correlated between cores.

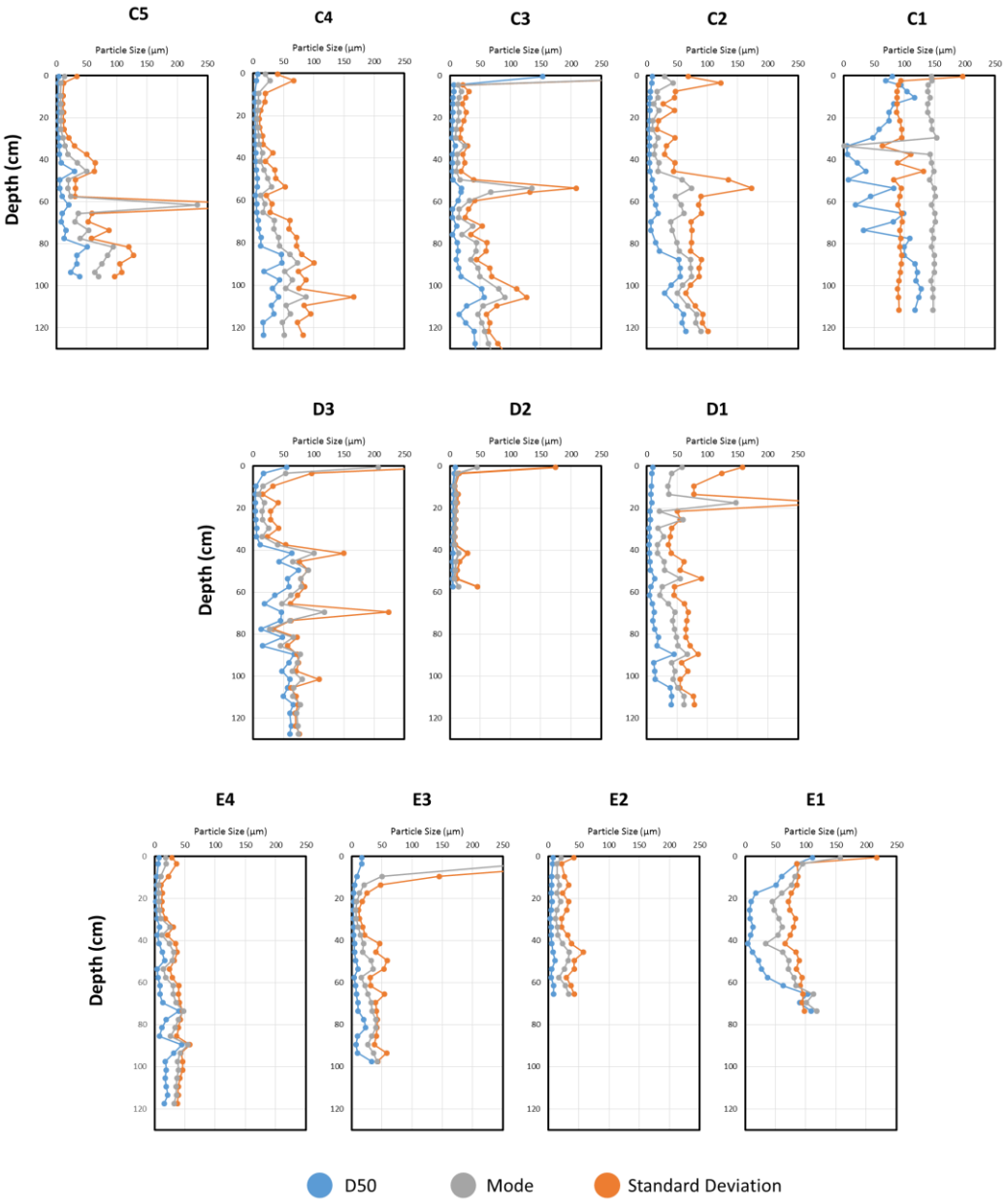

Figure 5. Profiles of grain size measured within each core. Blue line indicates the average d50 grain size measured at the sampled interval. Grey line indicates average mode of grain sizes measured at the sampled interval. Orange line indicates the standard deviation in grain sizes at the sampled interval.

Core	Approx. TRIV Depth (m)	Sedimentation rate ^{210}Pb (cm yr $^{-1}$)	Estimated Hg 1940 Depth (cm)	Calculated 1940 depth from ^{210}Pb (cm)
C1	4.9	0.77	42.0	58.52
C2	22.2	0.85	57.0	64.60
C3	32.5	3.22	66.0	244.72
C4	31.3	0.91	58.0	69.16
C5	9.1	0.64	46.0	48.64
D1	14.5	0.97	62.0	73.72
D2	33.2	1.06	-	80.56
D3	7.8	0.55	46.0	41.80
E1	6.6	0.56	34.0	42.56
E2	14.6	0.72	52.0	54.72
E3	31.3	0.87	62.0	66.12
E4	31.1	0.79	49.0	60.04

Table 2. Summary of a) approximate depth of the coring location over the base of the TRIV, b) sedimentation rate derived from ^{210}Pb regression, c) R^2 coeffecient of deterinmation for sedimentation regressions, d) estimated depth of the 1940 chronohorizon from Hg concentration profiles, e) sedimentation rate calculated from 1940 horizon using thickness of sediment above the horizon, and f) depth at which maximum Hg concentration was measured.

4.4 ^{210}Pb Sedimentation Rates

Excess ^{210}Pb activity profiles show a high variability in sedimentation rates across Trinity Bay (Table 2). Uniform activity near the surface indicates mixing of surface sediment has occurred in approximately half of the sediment cores, though x-radiographs revealed that both physical mixing and bioturbation was present to some extent within all of the cores. Decadal accumulation rates were determined from linear regression of log excess activity ^{210}Pb profiles. Data points exhibiting a negative excess ^{210}Pb activity were removed from the regression calculation because a logarithm cannot be calculated for a negative number.

Sedimentation rates across Trinity Bay ranged from 0.55 cm yr^{-1} to 3.22 cm yr^{-1}. Along Transect C, sedimentation rates correlate with position relative to the TRIV, with the highest sedimentation rate of 3.22 cm yr^{-1} being found directly over the TRIV and lower sedimentation rates being found in areas progressively further away from the valley axis.

Core D2, collected directly over the TRIV along transect D, varied drastically from the other cores through all analyses. Intense sediment mixing of up to 30 cm depth not seen in other cores was also present at D2, marring the excess ^{210}Pb results and leaving few data points to create a regression and reducing the confidence in the measured sedimentation rate. The lowest measured sedimentation rate along transect D, 0.55 cm yr^{-1}, was found at the core furthest from the TRIV axis, D3. Sedimentation rates had a similar variability along transect E, ranging from 0.56 – 0.87 cm yr^{-1}, with the

lowest rate being found closet to shore and the highest rate being found directly over the TRIV.

Evidence of sediment remobilization in Trinity Bay was abundant throughout all collected sediment cores, as indicated by the oscillating nature of the excess ^{210}Pb activity. This heavy remobilization along with surface mixing created regression lines that were linear in nature but in some instances contained a weak R^2 value. This uncertainty is acknowledged and has been constrained through the use of both Hg concentration and excess ^{210}Pb activity to determine sedimentation rates.

4.5 Hg Concentration

Bulk Hg concentration profiles were comparable in all cores, with a peak in concentration at or near the surface, ranging from 36 – 73 ng g^{-1} and decreasing down to background concentrations of approximately 20 ng g^{-1} at depth. Background concentration of Hg was found to be slightly elevated in cores C1 and E1 at approximately 30 ng g^{-1}, both of which contained successions with coarser sediment. Another exception to this trend is core D2 which is located centrally in the bay. Hg concentration at D2 is relatively uniform at approximately 50 ng g^{-1} from the surface to a depth of 40 cm, at which point the concentration drastically increases to approximately 100 ng g^{-1}, which is also the highest concentration measured in any of the cores. The historical 1960's contamination peak and subsequent fall in concentration observed in

previous studies, such as Santschi et al. (2001) and Al Mukiami (2016), could not be seen in Hg profiles of sediment cores collected within Trinity bay.

Chronohorizons can be visually determined on Hg profiles and can be compared between cores that lie on the same transect across the bay. When a visual correlation of the 1940 Hg concentration increase is made along transect C, a lowering of depth of occurrence is seen within cores that were collected closer to the TRIV's axis compared to the cores that were collected further away (Fig. 6). Transect E deviates only slightly from this pattern with the 1940 horizon being reached at a shallower depth than expected at location E4, given the valley's depth at this location. Core C1 and E1 are sand dominated and appear to have a higher background concentrations of Hg than the other cores which may be an artifact of sieving the coarse fraction in these cores. In any case, the 1940 horizon is found much shallower than in the other cores and, although the correlations are more tenuous, they appear to indicate an overall shallowing of the entire sequence, which is consistent with the core locations being further from the TRIV. These correlations are based off a visual interpretation alone, and are corroborated by the sedimentation rates measured at each coring location.

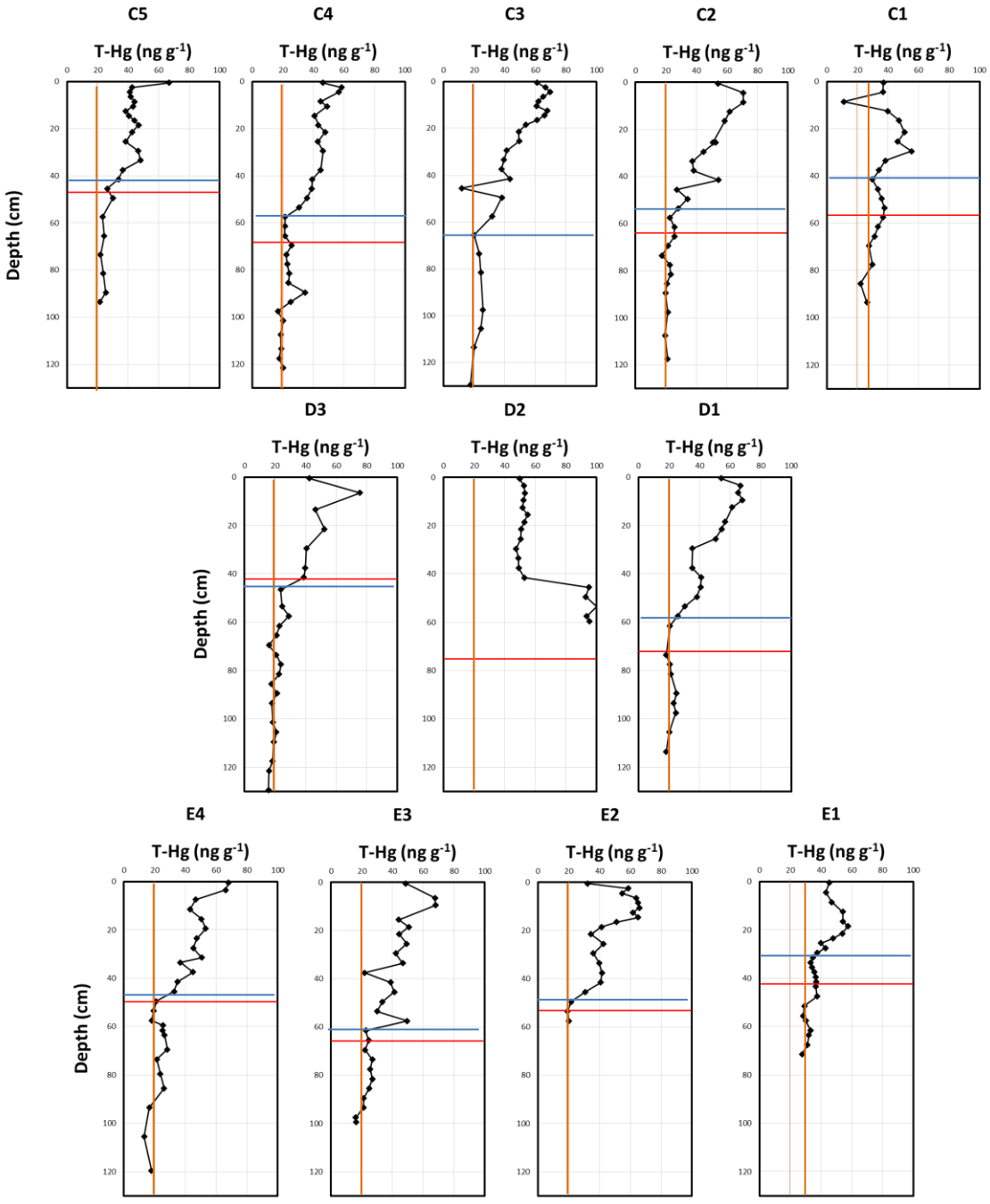

Figure 6. Profiles of total Hg concentration measured at sampled intervals at each coring location. Estimated background concentration represented by orange line (~20 ng g^{-1} or ~30 ng g^{-1} in C1 and E1). Red line indicates the year 1940 from ^{210}Pb sedimentation rates. Blue line indicates visual determination of the same 1940 chronohorizon.

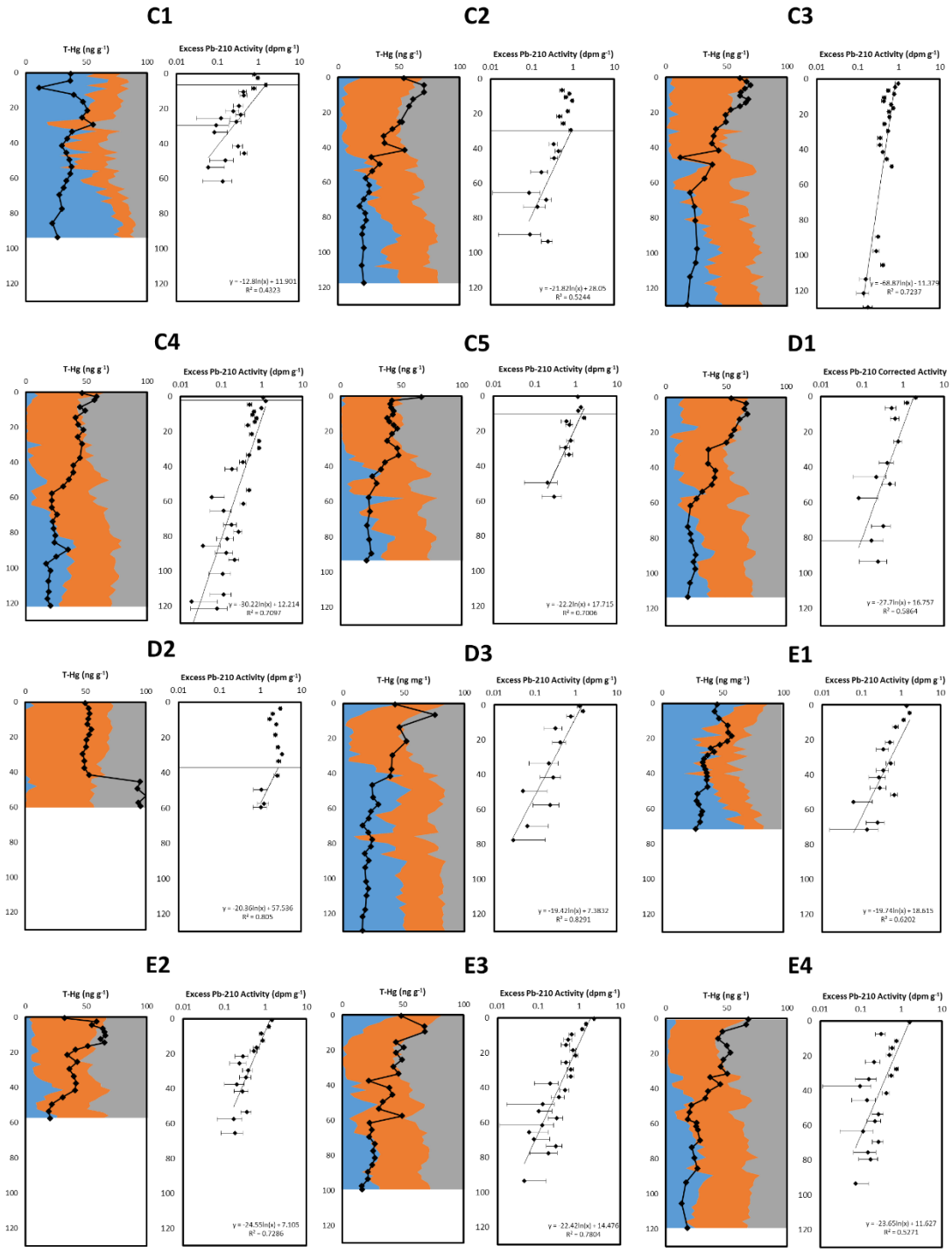

Figure 7. Summary of data from each coring location consisting of percent grain composition, where blue = sand (>65 μm), orange = silt (65 – 4 μm), and grey = clay (<4 μm), overlain by Hg concentration profiles and displayed next to excess ^{210}Pb profiles.

5. DISCUSSION

5.1 Sedimentation Rates

Sediment cores collected along transects of Trinity Bay revealed variable sedimentation rates, with the highest rates (0.55 – 3.22 cm yr^{-1}, Table 2) being directly over the TRIV. Sedimentation at one of the most central locations, core C3 (3.22 cm yr^{-1}), was more than three times as high as adjacent cores, cores C2 (0.84 cm yr^{-1}) and C4 (0.94 cm yr^{-1}), and more than four times as high as cores collected further away on the same transect, cores C1 (0.77 cm yr^{-1}) and C5 (0.64 cm yr^{-1}). The distance between core C3 and C4 is approximately 700 m, showing that within the same sedimentary environment, drastic changes in sedimentation rates can be found over relatively short distances. Sedimentation was also generally higher along transect C than the other two transects, which could be in part due to its location closer to the mouth of the Trinity River. Sedimentation within Trinity Bay appears to be affected by shoreline erosion, with elevated rates of sedimentation found nearshore along with higher sand concentrations in sediment than other more central cores.

In order to conclude the accuracy of sedimentation rates with certainty, excess ^{210}Pb in the sediment must be measured from the surface down to the depth at which background levels are reached (Fig. 7). This depth was not reached in all cores, adding a small amount of uncertainty to the regression analyses. Deeper sediment cores would be required to confirm these results. Calculation of sedimentation rates in this study also

assumed a linear sedimentation rate over the last decade. Given the damming history of the Trinity River, this assumption is likely not accurate. Though, it is also likely that regional sedimentation would be affected similarly to any decrease in sediment input due to sediment capture from upstream dams, making a relative comparison of sedimentation rates within the bay still valid. The majority of the decrease in sedimentation would have occurred between 1954 and 1968 with the construction of the Lake Anahuac and Lake Livingston dams (Ravens et al., 2009). A more accurate assumption of sedimentation rates would be to draw a second rate from this time interval to the present, which would likely reveal two distinct rates over time. Unfortunately, the collected data did not permit the location of this time interval nor did there appear to be two distinct slopes present in excess activity regressions.

A drastically higher sedimentation rate was measured at core C3, a rate that was not supported by Hg concentrations within the core. This high rate may be the result of calculating the excess ^{210}Pb activity regression while assuming no surface mixing had occurred. Upon further inspection, an argument could be made that mixing has indeed occurred. Re-calculating the regression from a point below the potential mixing layer would limit the data to six measured points at the base of the core. This new regression would present a lower sedimentation rate but our confidence in the measurement would be weak due to the few data points available.

All other sedimentation rates constructed from excess ^{210}Pb activity were supported by bulk Hg concentration profiles. In general, Hg profiles in all cores revealed a distinct point where Hg concentration drastically rises to approximately 40 ng g^{-1} and

is inferred as being the 1940 chronohorizon (Fig. 6). In cores with higher measured sedimentation rates, this horizon is reached at a deeper depth, which would be indicative of a higher accumulation rate coupled with compaction. This trend is present in all cores. The shallower occurrence of most of the visually determined 1940 horizons within Hg profiles when compared to a calculated 1940 horizon from excess ^{210}Pb sedimentation rates also provides evidence against the linear sedimentation rate assumption. Most profiles showed a peak in Hg concentration at or near the surface. At other locations within Galveston Bay, this peak has been considered to correlate to the 1960's chrono-horizon, but due to its shallow appearance in Trinity Bay, it is not considered as such in this study, unless it is to be assumed that sedimentation within Trinity Bay virtually ceased after the period of major dam construction along the Trinity River. The sedimentation rates found within this study do not support this conjecture, and from this we conclude that Hg alone is not enough to infer sedimentation rates within Galveston Bay.

While initially, results appear to confirm the hypothesis that sedimentation is increased due to position over the TRIV, all contributing factors must be taken into consideration. Visualizing core locations over a map of historical oil wells and pipelines reveals a trend of increasing sedimentation towards centers of past oil exploration (Fig. 8), particularly over transects C and D. Specific production information is not readily available to the public regarding many wells in the Trinity bay area, though all indications point towards the field only having minor production beginning in the 1950s. This can be compared to the Goose Creek oil field, located near the mouth of the SJR in

the northern portion of Galveston Bay, which has seen extensive production throughout the last century and experienced approximately 91 cm between 1918 and 1926 (Coplin and Galloway, 1999). This rate was localized and did not extend far from the wells. Even though production at the Trinity Bay oil field was likely much more limited and consisted of far fewer wells, it is possible that related construction within the bay could cause an anthropogenic increase in sedimentation through the resuspension of sediment. It is difficult to constrain the impact on sedimentation rates from human activity since enhanced sedimentation coincides with both the TRIV and historical oil and gas exploration. However, Transect E is located the furthest from wells and pipelines and shows a similar pattern of enhanced sedimentation over the TRIV, providing evidence that sedimentation is still being enhanced from subsidence stemming from differential compaction of the TRIV.

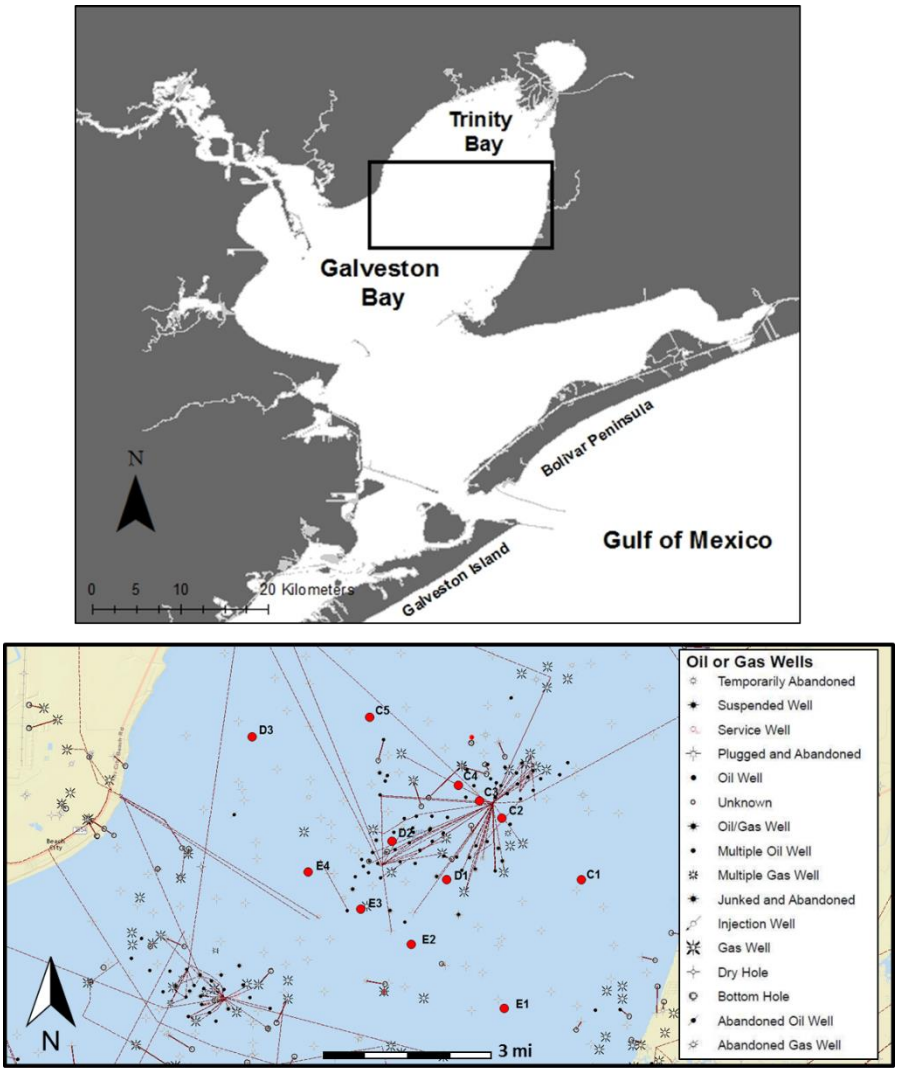

Figure 8. Map of Galveston Bay and surrounding area (top) with zoomed in view of study area (bottom). Sediment core locations indicated by red dots alongside oil and gas well infrastructure.

5.2 Subsidence

Given the high measured sedimentation rates, Trinity Bay could not have continued to exist as an estuary since its formation without an equally high rate of subsidence occurring. With average global sea-level rise occurring at a rate of approximately 0.20 cm yr^{-1}, sea-level rise would be quickly outpaced when compared to even the lowest sedimentation rate of 0.55 cm yr^{-1} measured in Trinity Bay. The relatively flat bathymetry of Trinity Bay gives credence to the claim that high rates of sedimentation coincide with higher rates of subsidence.

The lowest rate of sedimentation found within Trinity Bay was 0.55 cm yr^{-1} and contrasts with rates closer to 0.30 cm yr^{-1} found in portions of West Galveston Bay where subsidence is thought to be minimal (Al Mukaimi, 2016; Laverty, 2014). Using 0.30 cm yr^{-1} as the sedimentation expected to be found in an area of minimal regional subsidence and assuming the rate of subsidence in Galveston Bay increases linearly with sedimentation rate, we find that subsidence can be elevated by up to a factor of 10 directly over the TRIV and is elevated in general within Trinity Bay. However, variation in sedimentation rates along transects of Trinity Bay provide evidence that the TRIV is not compacting at equal rates throughout, so estimations of subsidence based solely on location over the TRIV may not be accurate. Limitations to the assumption that enhanced sedimentation coincides with enhanced subsidence also exist. Other areas in Galveston Bay have been documented as experiencing a higher rate of subsidence but not an equally high rate of sedimentation (Laverty, 2014). This can likely be attributed to

a diminished sediment supply in those areas. Use of our assumption should be limited to areas north of the Texas City Dyke where sediment is being retained.

The Pier 21 tidal gauge is located over the slope of the TRIV. Removing average eustatic sea-level rise (~0.2 cm yr^{-1}) from the RSLR rate measured at Pier 21 leaves us with 0.45 cm yr^{-1} of unaccounted for sea-level rise at Pier 21, which can be attributed to subsidence. Cores collected from Trinity Bay over a similar position to the slope of the TRIV as the Pier 21 tidal gauge measured sedimentation rates ranging from 0.72 – 0.97 cm yr^{-1} and we conclude that subsidence at these locations is occurring at a similar rate. Higher estimations of subsidence within Trinity Bay may reflect rapid compaction of surface sediments upon accumulation, whereas the Pier 21 tidal gauge would not reflect compaction of surficial sediments. Evidence still indicates that subsidence measured at Pier 21 reflects an enhanced rate stemming from its location over the TRIV, yet is also likely that fluid extraction would contribute slightly to the measured rate at this location due to its proximity to a subsidence epicenter near Texas City. Furthermore, the trend in subsidence due to location over the TRIV suggests that subsidence could be further enhanced east of Pier 21, where Galveston Island directly overlies the deepest portion of the TRIV.

Differential rates of compaction within the TRIV stem from variability in sediment type at depth. Coarser grain sediment along with harder substrates (buried oyster reefs) would be expected to compact less. Sediment composition from the surface to the base of all sediment cores appeared to be similar in composition in this study, but Anderson et al. (2005) documents variability in the composition of central basin

Holocene strata at depth within the TRIV. This suggests that elevated compaction within strata below 1.5 m within the TRIV is occurring and that this compaction of deeper strata, or lack thereof, is the source of much of the variability in sedimentation rates found within this study.

5.3 Implications

Given evidence presented here, areas directly overlying the TRIV, such as portions of Galveston Island and Bolivar Peninsula, are at a greater risk of tidal inundation and flooding due to shallow sediment compaction than areas that are outside of the TRIV. While much of Galveston Island has been built up to protect its large resident population, much of Bolivar Peninsula is composed of low lying coastal wetland and marsh. Wetlands provide not only a habitat for coastal communities but also natural protection against storm surges for more inland areas (Ravens et al., 2009). Enhanced RSLR will be observed first as rapid loss of wetlands, which is already being documented in Galveston Bay (Ravens et al., 2009), followed by enhanced shoreline erosion and eventually inundation of inland areas.

Alternatively, areas of Galveston Bay outside of the TRIV and away from regional subsidence hotspots may be at a much lower risk of flooding than previously thought. A regional rate of subsidence derived from the Pier 21 tidal gauge has often been used to characterize Galveston Bay as a whole. This rate should now be used with caution, as evidence suggests subsidence is highly variable across Galveston Bay.

The TRIV is only one of many incised valleys along the Texas coast, including Sabine, Lavaca, and Baffin Incised Valleys, all of which share similar structure, depth, and sedimentary composition (Anderson et al., 2015). Conclusions from this study carry through to these other valleys and it is hypothesized that similarly high rates of sedimentation, and therefore subsidence could be measured at each location. Similar to the TRIV, the Baffin and Lavaca incised valleys also run underneath part of Texas' barrier island system. Due to the rapid rates of modern sea level rise, barrier islands along the Texas coast are fragile and under constant threat of inundation during hurricanes. Subsidence from incised valleys increases the risk of losing portions of this barrier system during storm events. Texas's barrier islands, which extend from South Padre Island to Bolivar Peninsula, play a significant role in protecting the mainland from the full destructive force of the ocean. Monitoring future subsidence is paramount in the continued protection of Texas' coast and would additionally aid in the forecast of future sea-level rise by accounting for subsidence in predictive models. This could also help remove uncertainties in tidal gauge measurements, helping us to better understand past sea-level rise and the isostatic behavior of the Texas coast.

6. CONCLUSIONS

By using sedimentation as a proxy for subsidence, evidence of increased compaction of shallow Holocene sediments is observed over the TRIV. This compaction is found to be highly variable and localized, with the highest rates over the valley thalweg, decreasing to minimal levels outside the valley. However, this trend may be enhanced by anthropogenic activity and rates may not reflect only natural compaction of shallow sediments over the TRIV, but of deep seated compaction from fluid extraction.

Sedimentation rates over the TRIV were found to be approximately two to five times higher in areas directly over the valley than in areas outside. Subsidence is estimated to be similarly enhanced in areas over the TRIV than adjacent to it. The cause of this subsidence is may be due to a combination of subsidence factors, including fluid extraction and shallow sediment consolidation. The assumption that rates of sedimentation and subsidence correlate can only be safely made for areas of similar sediment input. While limited in its scope, evidence presented in our study also suggests that subsidence rates derived from the Pier 21 tidal gauge reflect a very localized subsidence and do not reflect regional rates, as the rate is currently and widely considered.

This study serves to shed light on marine sedimentary processes from within Trinity Bay that could have greater implications along the Texas Coast given the predicted increase in sea-level rise set to occur in the near future (IPCC, 2013). Subsidence rates must be reconsidered both regionally and locally along the upper Texas

coast in light of the role differential compaction of Holocene sediment may play in generating higher rates of subsidence over incised valley.

REFERENCES

Al Mukaimi, M., (2016). Geochemical and sedimentary record of urbanization and industrialization of the Galveston Bay watershed. Unpublished Ph.D. dissertation, Department of Oceanography, Texas A&M University, College Station, TX.

Al Mukiami, M., Dellapenna, T. M., and Williams, J., in review. Impacts of enhanced land subsidence on Galveston Bay, Texas: interactions between sediment accumulation rates and relative sea level rise. Submitted to Estuarine Coastal and Shelf Science.

Anderson, J.B., (2007). The Formation of the Upper Texas Coasts: A Geologist Answers Questions about Sand, Storms & Living by the Sea (Vol. 11). Texas A&M University Press.

Anderson, J. B., Wallace, D. J., Simms, A. R., Rodriguez, A. B., Weight, R. W., and Taha, Z. P. (2015). Recycling sediments between source and sink during a eustatic cycle: Systems of late Quaternary northwestern Gulf of Mexico Basin. Earth-Science Reviews, 153, p. 111-138

Appleby, P.G. and Oldfield, F., (1978). The calculation of lead-210 dates assuming a constant rate of supply of unsupported lead-210 to the sediment. Catena 5:1-8.

Bank, M. S., (2012). Mercury in the Environment: Pattern and Process. University of California Press, London, England.

Blum, M.D., Morton, R.A., and Durbin, J.M., (1995). ‘‘Deweyville’’ terraces and deposits of the Texas Gulf coastal plain: Gulf Coast Association of Geological Societies, Transactions, 45, p. 53-60.

Blum, M.D. and Price, D.M., (1998). Quaternary alluvial plain construction in response to glacio-eustatic and climatic controls, Texas Gulf coastal Plain.

Coplin, L.S. and Galloway, D., (1999). Houston-Galveston, Texas managing coastal subsidence, in: Galloway, D., Jones, D.R., Ingebritsen, S.E. (Eds.), Land subsidence in the United States. U.S. Geological Survey Circular 1182, 35-48.

Cox, D. T., Tissot, P., and Michaud, P. (2002). Water level observations and short-term predictions including meteorological events for entrance of Galveston Bay, Texas. Journal of Waterway, Port, Coastal, and Ocean Engineering, 128(1), 21-29.

Dellapenna, T.M., Kuehl, S.A., and Schaffner, L.C., (1998). Sea-bed mixing and particle residence times in biologically and physically dominated estuarine systems: a comparison of lower Chesapeake Bay and the York River subestuary. Estuarine Coastal and Shelf Science 46, 777-795.

EPA (Environmental Protection Agency) (1998), Method 7473: Mercury in Solids and Solutions by Thermal Decomposition, Amalgamation, and Atomic Absorption Spectrophotometry, EPA SW-846 Cincinnati, USEPA Office of Research and Development Environmental Monitoring Systems Laboratory.

Ewing, T.E., (1985). Subsidence and surface faulting in the Houston- Galveston area, Texas? Related to deep fluid withdrawal. In: DORFMAN, M.H., and Morton, R.A. (eds.), Geopressured-Geothermal Energy: Proceedings of the 6th U.S. Gulf Coast Geopressured-Geothermal Energy Conference. New York: Pergamon Press, pp. 289-298.

HGSD, (2008). Houston Galveston Subsidence District-Subsidence: 1906–2000. Available at http://www.subsidence.org/Assets/PDFDocuments/.

IPCC, (2013). Summary for Policymakers, in: Stocker, T.F., D. Qin, G.K. Plattner, M. Tignor, S.K. Allen, J. Boschung, A. Nauels, Y. Xia, Bex, V., Midgley, P.M. (Eds.), Climate Change 2013: The Physical Science Basis. Contribution of Working Group I to the Fifth Assessment Report of the Intergovernmental Panel on Climate Change. Cambridge University Press, Cambridge, United Kingdom and New York, NY, USA.

Koide, M., Soutar, A., and Goldberg, E.D., (1972), Geochronology with Pb-210. Earth Planet. Sci. Letters., 14, pp. 442-446.

Kolker, A.S., Allison, M.A., and Hameed, S., (2011). An evaluation of subsidence rates and sea-level variability in the northern Gulf of Mexico. Geophys. Res. Letters, 38.

Krishnaswamy, D. Lal., Martin, J., and Meybeckm, M, (1971). Geochronology of lake sediments. Earth Planet. Sci. Letters 11, pp. 407-414.

Langford, R.R., Clark, H.C., Warme, J.E., and Rehkemper, L.J. (1969). Galveston Bay estuarine system--Case study. Galveston, Texas, Gulf University Research Corp.

Laverty, P., (2014). Topographic and Base-level Control on Back-Barrier Lagoon Evolution: West Galveston Bay, TX, Department of Oceanography. Texas A&M University, thesis.

Lester, J. and Gonzalez, L. (2002). The State of the Bay, A Characterization of the Galveston Bay Ecosystem. The Galveston Bay Estuary Program (GBEP T-7).

Liu, G., Cai, Y., and O'Driscoll, N. (2012). Environmental chemistry and toxicology of mercury. John Wiley & Sons, Inc, USA.

Michel, T. A. (2006). "100 Years of groundwater use and subsidence in the Upper Texas Gulf Coast." Aquifers of the Gulf Coast of Texas. Texas Water Development Board, Austin: 139-148.

Morton, R.A., Blum, M.D., and White, W.A., (1996). Valley fills of incised coastal plain rivers: Gulf Coast Association of Geological Societies, Transactions, 46, p. 321–331.

NOAA (2013). Mean Sea Level Trend 8771450 Galveston Pier 21, Texas. Center for Operational Oceanographic Products and Services. Available at http://tidesandcurrents.noaa.gov/sltrends/sltrends_station.shtml?stnid=8771450.

Ravens, T. M., Thomas, R. C., Roberts, K. A., and Santschi, P. H. (2009). Causes of salt marsh erosion in Galveston Bay, Texas. Journal of Coastal Research, 265-272.

Rehkemper, L.J., (1969). Sedimentology of Holocene estuarine deposits, Galveston Bay. In: Holocene Geology of the Galveston Bay Area. Houston Geological Society, 1252.

Robbins, J.A, (1978). Geochemistry and geophysical application of radioactive lead. Pp. 285-393 in: J.O. Nriagu (ed.) The Biochemistry of lead in the environment. Elsevier, Amsterdam.

Rodriguez, A.B., Anderson, J.B., and Simms, A.R., (2005). Terrace Inundation as an Autocyclic Mechanism for Parasequence Formation: Galveston Estuary, Texas, U.S.A. Journal of Sedimentary Research 75, 608-620.

Santschi, P.H., Presley, B.J., Wade, T.L., Garcia-Romero, B., and Baskaran, M. (2001). Historical contamination of PAHs, PCBs, DDTs, and heavy metals in Mississippi River Delta, Galveston Bay and Tampa Bay sediment cores. Mar. Environ. Res. 52(1), 51-79.

Tebaldi, C., Strauss, B. H., and Zervas, C. E. (2012). Modelling sea level rise impacts on storm surges along US coasts. Environmental Research Letters, 7(1), 014032.

Thomas, M.A., and Anderson, J.B., (1994). Sea-level controls on the facies architecture of the Trinity/Sabine incised-valley system, Texas continental shelf, in Dalrymple, R.W., Boyd, R., and Zaitlin, B.A., eds., Incised-Valley Systems: Origin and Sedimentary Sequences: SEPM, Special Publication 51, 63–82.

Turner, R. E. (1991). Tide gauge records, water level rise, and subsidence in the northern Gulf of Mexico. Estuaries, 14(2), 139-147.

USGS, (2002). Houston-Galveston Bay Area, Texas, From Space - A New Tool for Mapping Land Sub, USGS Fact Sheet 110-02. Available at http://pubs.usgs.gov/fs/fs-110-02/pdf/FS_110-02.pdf.

White, W. and Morton, R. (1997). Wetland Losses Related to Fault Movement and Hydrocarbon Production, Southeastern Texas Coast. Journal of Coastal Research, 13(4), 1305-1320.

White, W.A., Morton, R.A., and Holmes, C.W., (2002). A comparison of factors controlling sedimentation rates and wetland loss in fluvial-deltaic systems, Texas Gulf coast. Geomorphology 44, 47-66.